

ation that the surface temperature of the sample was probably different from the temperature in deeper layers and that the response time of the whole system was about 0.5 s, the relatively large overshoots seen in the on/off mode (Fig. 3) can be understood. However in the pulsed mode, the refinement of power control (by repetition rate) leads to much smaller overshoots (Fig. 4).

V. SUMMARY

In this work we demonstrated that an IR fiber-optic radiometer is an accurate, simple, linear, and fast response device that can be used as a noncontact temperature sensor in a MW heating control system. Using this fiber-optic-based radiometer system, we succeeded in stabilizing a temperature of about 42°C with a standard deviation of $\pm 0.15^\circ\text{C}$ in a microwave heating environment. This specific temperature was chosen because of its relevance in medical applications. Control at higher temperatures presents less of a problem because the infrared emission is much stronger. The control method described here is novel, and it is potentially very useful for medical and industrial applications.

ACKNOWLEDGMENT

The authors wish to thank A. Yekuel, A. Levite, and B. Bar for their help and F. Moser for very valuable discussions.

REFERENCES

- [1] R. G. Olsen and T. D. David, "Hypothermia and electromagnetic rewarming in the rhesus monkey," *Aviat. Space. Environ. Med.*, pp 1111-1117, Dec 1984.
- [2] L. J. Anghileri and J. Robert, Eds., *Hyperthermia in Cancer Treatment*, vols. I-III. Boca Raton, FL: CRC Press, 1986.
- [3] A. Zur *et al.*, "Improved infrared fiberoptic radiometer for thermometry in electromagnetic induced heating," *Proc. SPIE*, vol. 1067, pp 75-82, 1989.
- [4] A. Katzir, H. F. Bowman, Y. Asfour, A. Zur, and C. R. Valery, "Infrared fibers for radiometer thermometry in hypothermia and hyperthermia treatment," *IEEE Trans. Biomed. Eng.*, vol. 36, pp. 634-637, 1989.
- [5] A. Zur and A. Katzir, "Fiber for low-temperature radiometric measurements," *Appl. Opt.*, vol. 26, pp. 1201-1206, 1987.
- [6] M. H. Sun, K. A. Wickersheim, and J. H. Kim, "Fiber optic temperature sensors in the medical setting," *Proc. SPIE*, vol. 1067, pp. 15-21, 1989.

InGaAsP DC-PBH Semiconductor Laser Diode Frequency Response Model

ALVARO AUGUSTO A. DE SALLES, MEMBER, IEEE

Abstract — A simple and accurate model for the frequency response of InGaAsP double-channel planar buried heterostructure semiconductor laser diodes intensity modulated in the microwave range is presented. It is shown that the parasitic capacitance associated with the reverse-biased blocking junction can significantly reduce the 3 dB modulation bandwidth. The results obtained and alternatives to improve the high-frequency performance are discussed and compared to experiments.

I. INTRODUCTION

InGaAsP double-channel planar buried heterostructure (DC-PBH) semiconductor laser diodes are important sources for optical communication systems operating at wavelengths of 1.3 and

Manuscript received August 15, 1989; revised November 1, 1989. This work was supported in part by TELEBRAS under Contract PUC-TELEBRAS 293/88.

The author is with the Catholic University of Rio de Janeiro, Rua Marques de São Vicente, 225, Gávea, CEP: 22453, Rio de Janeiro, RJ, Brazil.

IEEE Log Number 8934033

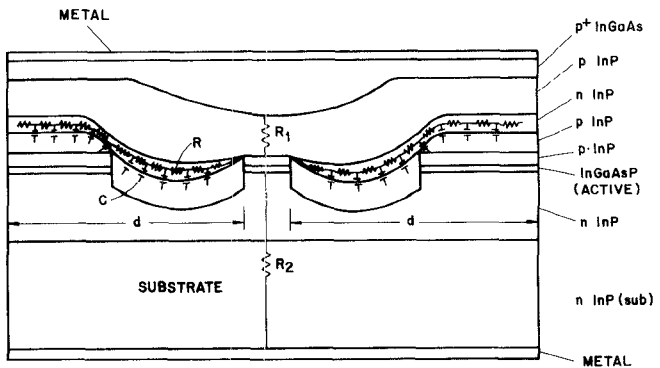


Fig. 1. Schematic structure for the InGaAsP DC-PBH laser

1.55 μm , where the dispersion and the losses in conventional optical fibers have their minima, respectively. Significant improvements in the static characteristics of these lasers have been obtained in the last decade, such as low threshold currents, high quantum efficiency, linearity of light versus current characteristic, operation at high optical power, and long-term reliability. One of the main reasons for this good static performance is the efficient lateral carrier confinement achieved when leakage current blocking junctions are produced outside the active region. In the InGaAsP DC-PBH lasers this is achieved by growing p-n-p-n layers in both sides of the active region. As a result, the p-n junctions reverse biased are very effective in reducing the static leakage current. However, the parasitic capacitance associated with the p-n junctions can significantly degrade the frequency response of these lasers when intensity modulated in the microwave range [1]-[6]. In order to achieve wide-band modulation, besides the optimization of the packaging parasitics and of some active region laser parameters [7]-[9], the parasitic capacitance must be decreased.

In this paper, an equivalent electrical circuit for the laser parasitics is described and its relevant parameters are estimated. Then, using a complete equivalent circuit for the intrinsic laser with its parasitics and using the SPICE 2G program, the DC-PBH laser frequency response is predicted and compared to measurements. The results obtained and ways to improve the high-frequency performance are discussed. These results can be useful for modulation bandwidth improvement of Fabry-Perot (FP) and distributed feedback (DFB) DC-PBH lasers.

II. LASER PARASITICS EQUIVALENT CIRCUIT AND FREQUENCY RESPONSE

The schematic structure of the InGaAsP DC-PBH laser ($\lambda \sim 1.3 \mu\text{m}$) is represented in Fig. 1. In this, the blocking junction distributed RC ladder network is also indicated.

The laser active region equivalent circuit suitable for nonlinear modeling has already been described by other authors [7]-[9]. Here, the equivalent circuit for the DC-PBH parasitics and its frequency response are described. The frequency response of the overall laser is a combination of the parasitic network and the intrinsic laser. The package (or mount) parasitics will be assumed negligible, since the lasers are expected to be mounted in microwave packages, with very large bandwidths. Under normal operating conditions the intrinsic laser is forward biased and the p-n junction between the upper n-InP layer and the p-InP layer below it is weakly reverse biased, reducing dc leakage current. The associated junction capacitance can be quite large as it usually extends across the entire area of the laser diode. This is

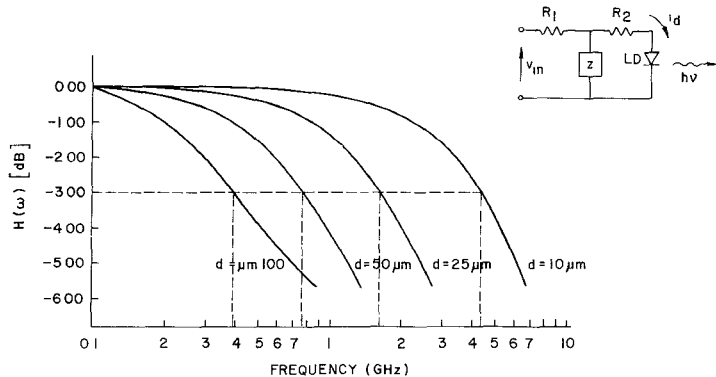


Fig. 2 Transfer characteristics $H(\omega)$ as a function of the parameter d for $N_A = 5 \times 10^{17} \text{ cm}^{-3}$ and laser parasitics equivalent circuit

the main impedance of these lasers. Input reflection coefficient measurements indicated that this capacitance can be as large as 100 pF when the blocking region half-width is around 100 μm . At high frequency, a parasitic current path follows the upper n-InP layer from the top contact and passes through the blocking junction capacitance to ground. Since the upper n-InP layer has a finite conductivity, this current path can be modeled as a ladder network of series resistances and parallel capacitances, as represented in Fig. 1 [3], [6]. These distributed resistances and capacitances contribute to a significant limitation for the intensity modulation bandwidth of the DC-PBH laser diode, as is shown below. Assuming that the blocking junction half-width is d , the impedance of the entire distributed RC ladder network is given by analogy to transmission line theory:

$$Z = \frac{Z_{in}}{2} = \frac{1}{2} \cdot Z_0 \cdot \frac{1 + e^{-2\gamma d}}{1 - e^{-2\gamma d}} = \frac{1}{2} \cdot Z_0 \coth(\gamma d) \quad (1)$$

where it is assumed that the RC ladder network is open circuited at the extremities of the laser chip. The $1/2$ factor appears because the input impedances of the distributed networks to both sides of the active region are associated in parallel. In (1), Z_0 is the characteristic impedance of the ladder network, given by

$$Z_0 = \left| \frac{R}{j\omega C} \right|^{1/2} \quad (2)$$

and γ is the "propagation constant":

$$\gamma = |j\omega RC|^{1/2}. \quad (3)$$

When the frequency is high enough so that the real part of γ is large, then the electric field does not penetrate too far beyond the lasing junction and the contribution of the distributed capacitance far away from the active region can be negligible. However, for the high impurity density normally used in the blocking layers, the conductivity is large and therefore the distributed series resistance is small. Then, the impedance Z strongly depends on the half-width d of the blocking layers [6]. This is responsible for the large roll-off and a small 3 dB bandwidth when d is large. For an abrupt heterostructure, the depletion layer p-n blocking junction distributed capacitance can be estimated from

$$C = L \left[\frac{q \cdot \epsilon \cdot N_B}{2(V_{bi} - V_a)} \right]^{1/2} \quad (4)$$

where L is the cavity length, ϵ is the permittivity, N_B is the doping density of the n or p side (depending on whether $N_A \gg N_D$, or vice versa), V_{bi} is the junction built-in potential, and V_a is the applied voltage ($V_a < 0$ for reverse bias). For the DC-PBH lasers, the donor doping density N_D of the upper n-InP layer is usually

much greater than the acceptor doping density N_A of the p-InP layer below it. Therefore, usually $N_B = N_A$. For the impurity concentrations normally used in the blocking junctions of these lasers, C is in the range $0.2\text{--}0.5 \text{ pF} \cdot \mu\text{m}^{-1}$ and R is around $0.1\text{--}0.2 \Omega \mu\text{m}^{-1}$.

For the laser parasitics frequency response estimation the simplified equivalent circuit shown in Fig. 2 is used. Here, Z is the impedance of the RC ladder network, and R_1 and R_2 are the parasitic series resistances. An estimation of the values of R_1 and R_2 can be made from the geometry and material used in the different layers, as well as from dc measurements. Typical values for R_1 and R_2 are around $1\text{--}2 \Omega$ and $2\text{--}3 \Omega$, respectively. The resistance R_2 can include the intrinsic laser series resistance, which is very small when it is biased above threshold [5], [7], [8]. Using standard circuit analysis, it can be easily shown that the laser parasitics frequency response is then estimated from the transfer function (Fig. 2)

$$H(\omega) = \frac{i_d}{V_m} = \frac{Z}{Z + R_2} \cdot \frac{1}{R_1 + \frac{Z \cdot R_2}{Z + R_2}}. \quad (5)$$

The transfer function $H(\omega)$ versus the parameter d is plotted in Fig. 2 for $N_A = 5 \times 10^{17} \text{ cm}^{-3}$. The results were calculated using the following parameters for the blocking junction: donor density and electron mobility in the n-InP layer, $N_d = 1 \times 10^{18} \text{ cm}^{-3}$ and $\mu = 1.8 \times 10^3 \text{ m}^2 \cdot \text{V}^{-1} \cdot \text{s}^{-1}$, respectively; InP intrinsic carrier concentration and dielectric constant, $n_i = 1 \times 10^8 \text{ cm}^{-3}$ and $\epsilon = 12.4$, respectively; thickness of n-InP layer $h = 0.9 \mu\text{m}$; laser diode cavity length $L = 300 \mu\text{m}$; and laser injection current $I_L = 1.2 I_{th}$ ($I_{th} = 14 \text{ mA}$). It can be seen from these curves that the cutoff frequency increases when the blocking region half-width d is reduced. This is due to the reduction of the area associated with the blocking junction capacitance. The cutoff frequency increases also when the acceptor doping density N_A in the p-InP layer just below the upper n-InP layer is reduced. This is again due to the reduction of the blocking junction capacitance, which is proportional to the square root of N_A , as is shown in (4). The blocking region half-width d reduction can be obtained by proton isolation or mesa etching [1]–[4].

III. INTRINSIC LASER AND OVERALL FREQUENCY RESPONSE

The intrinsic laser frequency response was modeled using the rate equations and SPICE 2G computer program, and the results for different dc bias currents are plotted in Fig. 3. The laser diode parameters used in these simulations are: electron lifetime $\tau_n = 1.5 \text{ ns}$; photon lifetime, 3 ps; electron density (at which $g = 0$) $N_0 = 10^{24} \text{ m}^{-3}$; gain constant $g_0 = 0.4 \times 10^{-12} \text{ m}^3 \text{ s}^{-1}$; optical confinement factor $\Gamma = 1$; fraction of spontaneous emission cou-

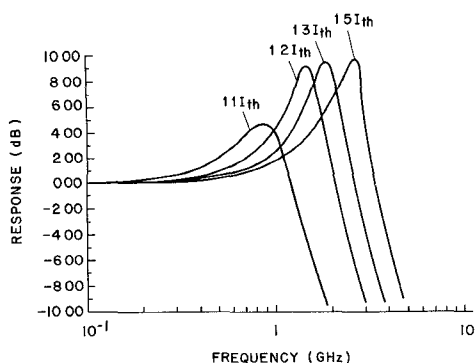


Fig. 3. Intrinsic laser frequency responses at different dc bias currents

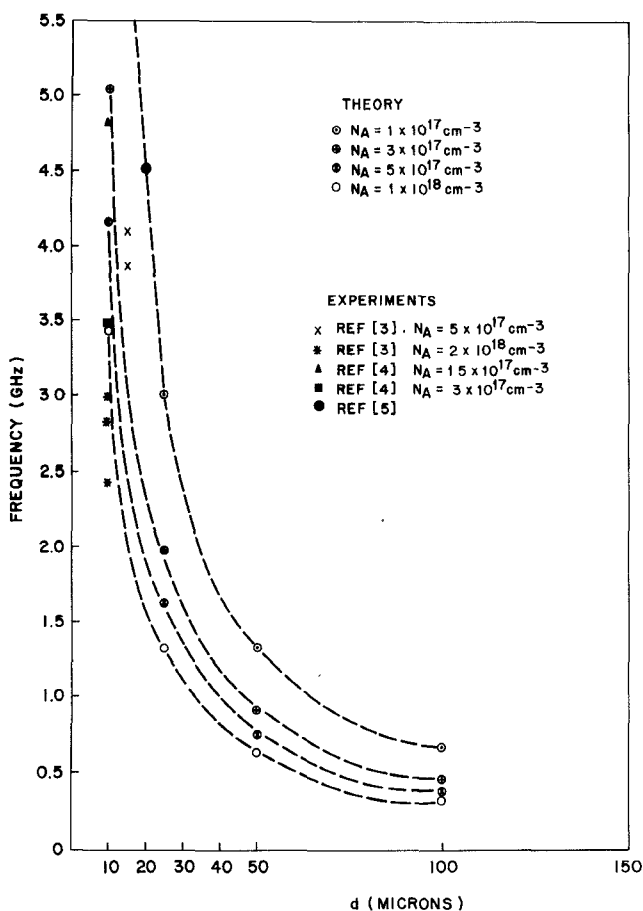


Fig. 4. Estimated 3 dB bandwidth of the overall network and some measured values

pled into lasing mode $\beta = 0.5 \times 10^{-3}$; gain compression factor $\epsilon = 6.7 \times 10^{-24} \text{ m}^2$; active region volume $V = 7.2 \times 10^{-17} \text{ m}^3$; and laser threshold current $I_{th} = 14 \text{ mA}$. A simple computer program has been developed to calculate the overall frequency response of the intrinsic laser and its parasitics. The estimated 3 dB bandwidth of the overall network as a function of the parameter d and for different values of N_A , together with some experimental values, are plotted in Fig. 4. It can be observed that the overall network cutoff frequencies (Fig. 4) are generally larger than those calculated for the laser parasitics themselves. This is due to the intrinsic laser resonant peak associated with relaxation oscillation (Fig. 3).

IV. COMMENTS AND CONCLUSIONS

A simple model for the DC-PBH laser parasitics and for the overall network frequency response was described in this paper and compared to certain measurements. It is shown that the blocking junction distributed capacitance can significantly degrade the frequency response of these lasers. The blocking junction half-width and the acceptor doping density reduction effects on the 3 dB modulation bandwidth increase are predicted. When the blocking junction half-width d is large ($d \sim 40\text{--}100 \mu\text{m}$) and for dc bias equal or greater than 30–50% above threshold, the intrinsic laser relaxation oscillation frequency is well above the laser parasitics cutoff frequency. Therefore, to improve the frequency response of the FP and DFB DC-PBH lasers, besides the optimization of the intrinsic laser parameters and the packaging parasitics, the blocking junction capacitance must be decreased.

ACKNOWLEDGMENT

The author is grateful to M. C. R. Carvalho, M. T. M. Rocco, G. F. B. Almeida, and J. S. Pereira for several contributions to this paper.

REFERENCES

- [1] I. D. Henning, "High speed transient effects in quaternary lasers," *Proc Inst Elec Eng*, vol. 131, pt. H, no. 3, pp. 133–138, June 1984.
- [2] I. Mito, M. Kitamura, M. Yamaguchi, and K. Kobayashi, "Single longitudinal-mode operation of DFB-DC-PBH LD under Gbit/s modulation," *Electron Lett*, vol. 20, no. 6, pp. 261–263, 15 Mar. 1984.
- [3] K. Kasahara, T. Terakado, A. Suzuki, and S. Murata, "Monolithically integrated high-speed light source using 1.3 μm , wavelength DFB-DC-PBH laser," *J Lightwave Technol*, vol. LT-4, pp. 908–912, July 1986.
- [4] P. P. G. Mols and J. A. van Steenwijk, "Accurate equivalent circuit model for small and large signal modulation behaviour of a laser diode up to gigahertz range," in *Proc 1987 European Conf. Opt. Commun.*, pp. 127–130.
- [5] J. Kamite *et al.*, "Analysis of the parasitic effective capacitance of buried-heterostructure lasers," *Electron Lett*, vol. 22, no. 8, pp. 407–409, 10 Apr. 1986.
- [6] K. Y. Lau and A. Yariv, "Ultra-high speed semiconductor lasers," *IEEE J Quantum Electron*, vol. QE-21, pp. 121–137, Feb. 1985.
- [7] R. S. Tucker and D. J. Pope, "Microwave circuit models of semiconductor injection lasers," *IEEE Trans Microwave Theory Tech*, vol. MTT-31, pp. 289–294, Mar 1983.
- [8] R. S. Tucker and I. P. Kaminov, "High-frequency characteristics of directly modulated InGaAsP ridge waveguide and buried heterostructure lasers," *J Lightwave Technol*, vol. LT-2, pp. 385–393, Aug 1984.
- [9] R. S. Tucker, "High-speed modulation of semiconductor lasers," *J Lightwave Technol*, vol. LT-3, pp. 1180–1192, Dec 1985.

Design and Applications of Optically Controllable Finline Structures

K. UHDE AND R. EIMERTENBRINK

Abstract—This paper describes the design of finline structures on a semiconducting substrate. Using high-resistivity silicon and gallium arsenide substrates, insertion losses between 1 dB and 2 dB have been achieved. By illuminating the slot region with a laser diode, attenuators and/or switches with on-off ratios up to –40 dB have been realized in the

Manuscript received July 14, 1989; revised November 14, 1989. This work was carried out at the Technische Universität Hamburg-Harburg, Arbeitsbereich Hochfrequenztechnik.

K. Uhde is with Valvo UB Bauelemente der Philips GmbH, Applikationslabor, Abt AT, Vogt-Kölln-Straße 30, D-2000 Hamburg 54, West Germany. R. Eimertenbrink is with Blaupunkt GmbH, Abt MC1-EAS4, Robert-Bosch-Str 200, 3200 Hildesheim, West Germany.

IEEE Log Number 8934031.